

CFD modelling of the galloping response of a 3:2 rectangular prism in smooth and turbulent flow

A. J. Álvarez^a, F. Nieto^b, K.C.S. Kwok^c, L. Patruno^d

^aCITEEC, University of A Coruña, A Coruña, Spain, antonio.jose.alvarez@udc.es

^bCITEEC, University of A Coruña, A Coruña, Spain, felix.nieto@udc.es

^cUniversity of Sydney, Sydney, NSW, Australia, kenny.kwok@sydney.edu

^dUniversity of Bologna, Bologna, Italy, luca.patruno@unibo.it

Summary

3D LES simulations of a rectangular prism of side ratio 3:2 have been conducted under smooth flow for static and dynamic cases. The dynamic case was allowed to oscillate in the heave degree of freedom, showing good agreement with available experimental data.

Keywords: galloping, 3D LES, 3:2 rectangular prism, energy harvester

1 INTRODUCTION

Energy harvesters are electromechanical devices designed for generating electrical energy from the vibrations of a body undergoing wind-induced excitation (Barrero-Gil et al. 2012; Zhang et al. 2020). These devices produce energy at lower wind speeds than wind turbines and are very compact, which make them suitable for urban environments (Poozesh et al. 2025). As rectangular prisms of small width to height ratio are prone to undergo galloping oscillations (Mannini et al. 2018) they are particularly suited for being the geometry producing the excitation of the energy harvester. In the following the study of dynamic response of a rectangular prism of side ratio 3:2 by means of 3D LES simulations is presented, in order to assess the used of CFD simulations as a reliable tool for predicting the performance of the energy harvester.

2 FORMULATION

The flow is modelled using the Large Eddy Simulation (LES) formulation. For solving the set of Navier-Stokes equations the open-source software OpenFOAM in the ESI v2212 (OpenFOAM 2022), by means of Yoshizawa's model (Yoshizawa 1986) which add a transport equation for the kinetic energy of the unresolved stresses, named as kEqn on OpenFOAM. The sign convention for the aerodynamic forces is shown in Figure 1a. The time dependent force coefficients (drag C_D , lift C_L and moment C_M) and Strouhal number are calculated as shown in Eq. (1).

$$C_D = \frac{F_D}{\frac{1}{2}\rho U_\infty^2 H}, \quad C_L = \frac{F_L}{\frac{1}{2}\rho U_\infty^2 H}, \quad C_M = \frac{M_P}{\frac{1}{2}\rho U_\infty^2 H^2}, \quad St = \frac{fH}{U_\infty}, \quad (1)$$

where H stands for the height of the prism, F_D , F_L and M_P are the drag and lift forces, and torsional moment per unit of span length, U_∞ is the incoming wind velocity, ρ is the air density, and f is the dominant frequency of the lift coefficient evaluated from a Fourier analysis. Symbols $\bar{\quad}$ and σ represent the mean and standard deviation respectively. In Eq. (2) the so-called Pope's (Pope 2004) criterium (M) is presented, which is used for assessing the quality of the LES simulations, considering well resolved LES simulations those featuring an energy content of the modelled scales

(subgrid scales, sgs) equal or below 20% (Chapman 1979; Pope 2004), hence $M(\mathbf{x}, t) \leq 0.2$.

$$M(\mathbf{x}, t) = \frac{k_{sgs}(\mathbf{x}, t)}{k(\mathbf{x}, t) + k_{sgs}(\mathbf{x}, t)}, \quad (2)$$

where $k_{sgs}(\mathbf{x}, t)$ is the turbulent kinetic energy of the unresolved scales, $k(\mathbf{x}, t)$ is the turbulent kinetic energy of the resolved scales. Hence, a well resolved LES simulation has $M(\mathbf{x}, t) \leq 0.2$ in the regions of interest of the simulation. The Scruton number (Sc) is used for characterising the dynamic properties of the harvester, which is calculated as indicated in Eq. (3).

$$Sc = \frac{4\pi m\xi}{\rho BHL}, \quad (3)$$

with m is the total mass of the model, ξ is the relative damping of the system and B , H and L are the dimensions of the prism.

3 COMPUTATIONAL MODELLING

Second order schemes have been used for approximating the advancement in time, the diffusive and convective terms. The pressure-velocity coupling was solved by means of the PIMPLE algorithm. The simulations were ran at a constant time-step providing a maximum Courant number below 1.0. The simulations under galloping include the Arbitrary Lagrangian Eulerian algorithm for accounting for the mesh motion. The prism was only allowed to move in the heave degree of freedom, and its oscillation was modelled as a single-degree-of-freedom mass-spring-damper system. The conventional serial staggered scheme was used for resolving the coupling between the fluid, structure and dynamic mesh. The mesh sizes for the different regions of the mesh were established following the procedure described in Nieto et al. (2025), achieving a $y^+ = 1.68$ for a mesh with 1925744 elements. A sketch of the fluid domain with its dimensions is shown in Figure 1b, and their values are presented in Table 1. The properties of the boundary layers are presented in Table 2. The values of Pope's criterium for the static simulation are shown in Figure 1c.

Table 1: Fluid domain dimensions.

Λx	Λy	$\mathcal{D}x$	$\mathcal{D}y$	$\mathcal{D}z$
$16.75H$	$16.5H$	$50H$	$34H$	$4H$

Table 2: Boundary layer mesh characteristics. (h_1 is the height of the elements in the first row of the boundary layer (bl), H_{bl} is the total height of the bl, n_{bl} is the number of rows of elements forming the bl, x_1 is the width of the elements in the first row of the bl, and gr_{bl} is the growth ratio between row heights in the bl)

h_1/H	H_{bl}/H	n_{bl}	x_1/h_1	gr_{bl}
1.119×10^{-3}	4.442×10^{-2}	9	2.84	1.35

When considering a turbulent inflow, turbulence synthetic methods were applied by using Syn-Inflow software (Patruno and de Miranda 2020)

4 RESULTS

In Table 3 the force coefficient values of the prism under smooth flow for a 0° angle of attack (AoA) are presented and compared with some available experimental data. The reported values are well aligned with the experimental data. On the other hand the results of the galloping simulations, which were conducted for a $Sc = 28$, AoA= 0° and considering two levels of turbulent intensity, are presented in Figure 1d. It can be seen that the obtained amplitudes of oscillation are in good agreement with the experimental results from Mannini et al. (2018), although they are presenting slightly higher values, which could be explained by the small discrepancies in the force coefficients and hence producing a different vertical force. Moreover the spanwise length of the prism, different in the simulations from the one tested, could also be playing a role in the observed differences.

Table 3: 3:2 rectangular prism force coefficients for smooth flow and 0° angle of attack (AoA). (PS refers to present study)

	Re_H	$\overline{C_d}$	$\overline{C_l}$	$\overline{C_m}$	$\widetilde{C_d}$	$\widetilde{C_l}$	$\widetilde{C_m}$	St
PS	143000	1.74	0.01	0.00	0.05	1.04	0.07	0.11
Mannini et al. (2016)	146800	1.75				0.81		0.11
Mannini et al. (2018)	143000	1.77	0.00					0.11

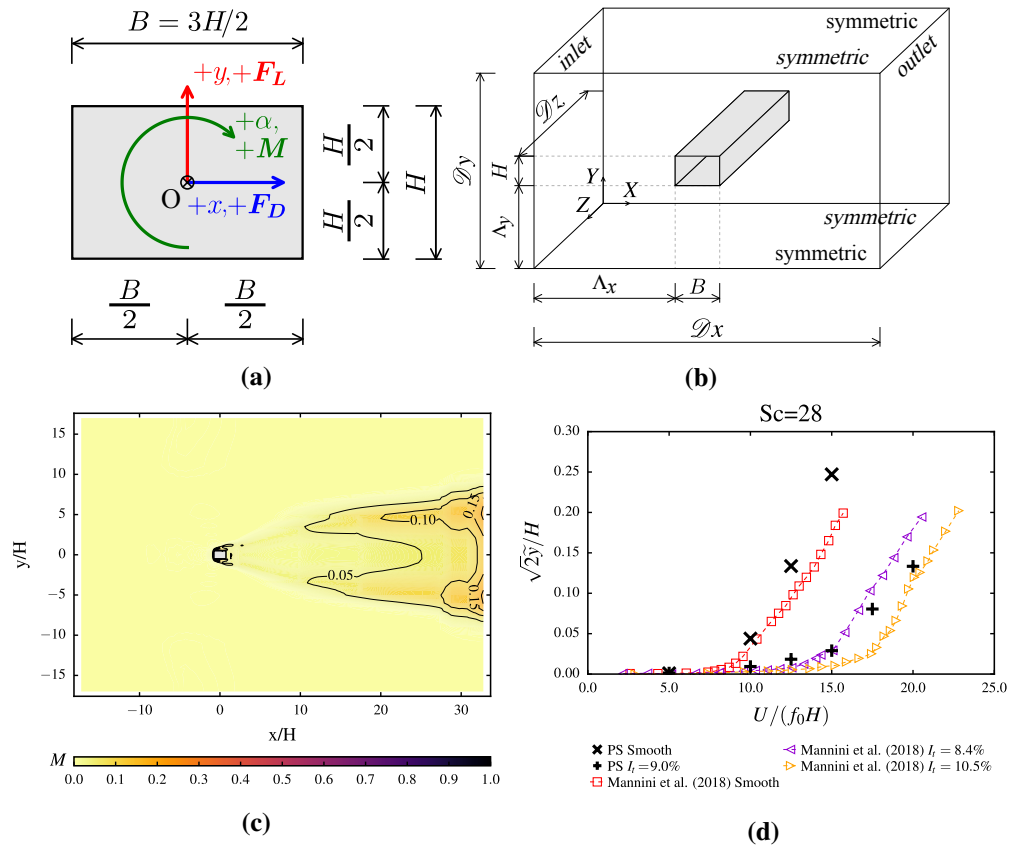


Figure 1: Fluid domain and results: (a) sign convention, (b) sketch of the overall fluid domain (not at scale), (c) Pope's criterion for the static simulation and (d) Equivalent sinusoidal amplitudes of heave oscillation under smooth flow.

5 CONCLUSIONS

In this study 3D LES simulations of the 3:2 rectangular prism under two different levels of turbulence intensity have been completed, being able to successfully reproduce the expected galloping behaviour of the prism and hence indicating that this kind of simulations could be a good predictor of the response of energy harvesters.

ACKNOWLEDGEMENTS

This work has been supported by grant TED2021-132243B-I00 funded by MICIU/AEI/10.13039/501100011033 and by European Union NextGenerationEU/PRTR. Funding has also been obtained from the Galician Regional Government through actions ED431C 2021/33 and ED431 2025/55. The computations have been carried out in the Galicia Supercomputing Centre (CESGA).

REFERENCES

- Barrero-Gil, A., Pindado, S., Avila, S., 2012. Extracting energy from vortex-induced vibrations: A parametric study. *Applied Mathematical Modelling* 36, 3153–3160. <https://doi.org/10.1016/j.apm.2011.09.085>.
- Chapman, D.R., 1979. Computational aerodynamics development and outlook. *AIAA Journal* 17, 1293–1313. <https://doi.org/10.2514/3.61311>.
- Mannini, C., Marra, A.M., Massai, T., Bartoli, G., 2016. Interference of vortex-induced vibration and transverse galloping for a rectangular cylinder. *Journal of Fluids and Structures* 66, 403–423. <https://doi.org/10.1016/j.jfluidstructs.2016.08.002>.
- Mannini, C., Massai, T., Marra, A.M., 2018. Unsteady galloping of a rectangular cylinder in turbulent flow. *Journal of Wind Engineering and Industrial Aerodynamics* 173, 210–226. <https://doi.org/10.1016/j.jweia.2017.11.010>.
- Nieto, F., Álvarez, A.J., Kowk, K.C.S., Patruno, L., 2025. Linkage between spatial resolution and accuracy in 3d les: three examples in bluff body aerodynamics, in: *Proceedings of the 9th European-African Conference on Wind Engineering (9EACWE)*, Trondheim, NOR. pp. 1–5.
- OpenFOAM, E.O., 2022. User Guide. Version v2212. Technical Report. ESI OpenCFD OpenFOAM.
- Patruno, L., de Miranda, S., 2020. Unsteady inflow conditions: A variationally based solution to the insurgence of pressure fluctuations. *Computer Methods in Applied Mechanics and Engineering* 363, 112894. <https://doi.org/10.1016/j.cma.2020.112894>.
- Poozesh, P., Álvarez, A., Nieto, F., 2025. Machine learning-based prediction of the performance of a wind-excited piezoelectric energy harvester deployed in urban environment. *Journal of Wind Engineering and Industrial Aerodynamics* 267, 106222. <https://doi.org/10.1016/j.jweia.2025.106222>.
- Pope, S.B., 2004. Ten questions concerning the large-eddy simulation of turbulent flows. *New Journal of Physics* 6. <https://doi.org/10.1088/1367-2630/6/1/035>.
- Yoshizawa, A., 1986. Statistical theory for compressible shear flows, with the application of subgrid modelling. *Physics of Fluids* 29, 155–163. <https://doi.org/10.1063/1.865552>.
- Zhang, M., Hu, G., Wang, J., 2020. Bluff body with built-in piezoelectric cantilever for flow-induced energy harvesting. *International Journal of Energy Research* 44, 3762–3777. <https://doi.org/10.1002/er.5164>.